J|A|C|S
ARTICLES
Published on Web 11/08/2002

Electronically Unsaturated Three-Coordinate Chloride and Methyl Complexes of Iron, Cobalt, and Nickel

Patrick L. Holland,* Thomas R. Cundari,*,†,‡ Lanyn L. Perez, Nathan A. Eckert, and Rene J. Lachicotte

Contribution from the Department of Chemistry, University of Rochester, Rochester, New York 14627, and Department of Chemistry and the Computational Research on Materials Institute, University of Memphis, Memphis, Tennesee 38152

Received January 14, 2002

Abstract: Three-coordinate organometallic complexes are rare, especially with the prototypical methyl ligand. Using a hindered, rigid bidentate ligand (L), it is possible to create 12-electron methyliron(II) and 13-electron methylcobalt(II) complexes. These complexes are thermally stable, and ^{1}H NMR spectra suggest that the low coordination number is maintained in solution. Attempts to create the 14-electron $LNiCH_3$ led instead to the three-coordinate nickel(I) complex LNi(THF). Single crystals of $LMCH_3$ are isomorphous with the new three-coordinate chloride complexes LNiCl and LCoCl. Along with the recently reported LFeCl (Smith, J. M.; Lachicotte, R. J.; Holland, P. L. *Chem. Commun.* **2001**, 1542), these are the only examples of three-coordinate iron(II), cobalt(II), and nickel(II) complexes with terminal chloride ligands, enabling the systematic evaluation of the effect of coordination number and metal identity on M−Cl bond lengths. Electronic structure calculations predict the ground states of the trigonal complexes.

Introduction

Three-coordinate complexes of the transition metals are rare, because it is difficult with only three ligand donors to reach preferred configurations with 16 or 18 electrons in the metal bonding and nonbonding orbitals. In all solution-phase three-coordinate transition metal complexes, the metal is protected with extremely bulky ligands. In this way, chemists have been able to stabilize three-coordinate[1] and even two-coordinate[2] metal centers; the ground-breaking work of Power is especially notable in the development of routes to three-coordinate late transition metal complexes.[3,4] However, the ligands that offer protection often block the metal from the interesting intermolecular reactivity expected from the unusual orbital structure of the low-coordinate metal. When reactivity is observed at three-coordinate metal sites, it can be spectacular. Work by Wolczanski and Cummins is illustrative, in which low-coordinate complexes of group 4−6 metals cleave C−H bonds of alkanes, the N−N bond of nitrous oxide, and triple bonds of CO, NO, and N_2.[5−8] The small HOMO−LUMO gap, coincidence of electrophilic and nucleophilic behavior, and attendant large binding constants for the fourth ligand are factors that contribute to this prodigious ability to activate organic and inorganic substrates.

Low coordination may also be used in nature to perform difficult bond-cleaving tasks: the iron−molybdenum cofactor of nitrogenase has six iron atoms of roughly trigonal planar geometry at its core (Figure 1).[9] Although there is no conclusive evidence that N_2 binds or is transformed at these iron atoms, biochemists, spectroscopists, and theoreticians have accumulated evidence that points toward substrate binding one or more of

* To whom correspondence should be addressed. E-mail: holland@chem.rochester.edu.
† University of Memphis.
‡ Current address: Department of Chemistry, University of North Texas, Box 305070, Denton, TX 76203.

(1) Reviews: (a) Cummins, C. C. *Prog. Inorg. Chem.* **1998**, *47*, 685−836. (b) Alvarez, S. *Coord. Chem. Rev.* **1999**, *193*−*195*, 13−41.
(2) (a) Power, P. P. *Comments Inorg. Chem.* **1989**, *8*, 177−202. (b) Power, P. P. *Chemtracts: Inorg. Chem.* **1994**, *6*, 181−195. (c) Ellison, J. J.; Ruhlandt-Senge, K.; Power, P. P. *Angew. Chem., Int. Ed. Engl.* **1994**, *33*, 1178−1180. (d) Wehmschulte, R. J.; Power, P. P. *Organometallics* **1995**, *14*, 3264−3267.
(3) (a) Murray, B. D.; Power, P. P. *Inorg. Chem.* **1984**, *23*, 4584−4588. (b) Murray, B. D.; Power, P. P. *J. Am. Chem. Soc.* **1984**, *106*, 7011−7015. (c) Hope, H.; Olmstead, M. M.; Murray, B. D.; Power, P. P. *J. Am. Chem. Soc.* **1985**, *107*, 712−713. (d) Olmstead, M. M.; Power, P. P.; Sigel, G. *Inorg. Chem.* **1986**, *25*, 1027−1033. (e) Ellison, J. J.; Power, P. P.; Shoner, S. C. *J. Am. Chem. Soc.* **1989**, *111*, 8044−8046. (f) Bartlett, R. A.; Ellison, J. J.; Power, P. P.; Shoner, S. C. *Inorg. Chem.* **1991**, *30*, 2888−2894. (g) Olmstead, M. M.; Power, P. P.; Shoner, S. C. *Inorg. Chem.* **1991**, *30*, 2547−2551. (h) Power, P. P.; Shoner, S. C. *Angew. Chem., Int. Ed. Engl.* **1991**, *30*, 330−332. (i) Chen, H.; Olmstead, M. M.; Pestana, D. C.; Power, P. P. *Inorg. Chem.* **1991**, *30*, 1783−1787.
(4) $[Fe(SC_6H_2tBu_3)_3]^-$: (a) MacDonnell, F. M.; Ruhlandt-Senge, K.; Ellison, J. J.; Holm, R. H.; Power, P. P. *Inorg. Chem.* **1995**, *34*, 1815−1822. (b) Sanakis, Y.; Power, P. P.; Stubna, A.; Münck, E. *Inorg. Chem.* **2002**, *41*, 2690−2696. (c) Agostic interactions in some low-coordinate iron thiolate complexes make higher coordinate descriptions more accurate: Evans, D. J.; Hughes, D. L.; Silver, J. *Inorg. Chem.* **1997**, *36*, 747−748.
(5) Neithamer, D. R.; LaPointe, R. E.; Wheeler, R. A.; Richeson, D. S.; Van Duyne, G. D.; Wolczanski, P. T. *J. Am. Chem. Soc.* **1989**, *111*, 9056−9072.
(6) (a) Cummins, C. C.; Baxter, S. M.; Wolczanski, P. T. *J. Am. Chem. Soc.* **1988**, *110*, 8731−8733. (b) Schafer, D. F.; Wolczanski, P. T. *J. Am. Chem. Soc.* **1998**, *120*, 4881−4882.
(7) Cummins, C. C. *Chem. Commun.* **1998**, 1777−1786 and references within.
(8) (a) Odom, A. L.; Cummins, C. C.; Protasiewicz, J. D. *J. Am. Chem. Soc.* **1995**, *117*, 6613−6614. (b) Veige, A. S.; Slaughter, L. M.; Wolczanski, P. T.; Matsunaga, N.; Decker, S. A.; Cundari, T. R. *J. Am. Chem. Soc.* **2001**, *123*, 6419−6420.
(9) (a) There are short Fe−Fe contacts of 2.65 ± 0.04 Å in the FeMoco that probably modify the behavior of iron: Mayer, S. M.; Lawson, D. M.; Gormal, C. A.; Roe, S. M.; Smith, B. E. *J. Mol. Biol.* **1999**, *292*, 871−891. (b) A very recent paper presents evidence that there is a fourth ligand coordinated to these iron atoms: Einsle, O.; Tezcan, F. A.; Andrade, S. L. A.; Schmid, B.; Yoshida, M.; Howard, J. B.; Rees, D. C. *Science* **2002**, *297*, 1696−1700.

10.1021/ja025583m CCC: $22.00

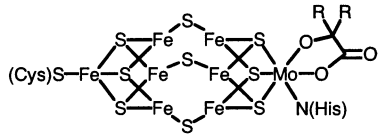

Figure 1. The iron−molybdenum cofactor of iron−molybdenum nitrogenase. Coordinates derived from ref 9a.

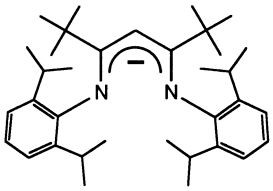

Figure 2. The β-diketiminate ligand used in this paper, L.

the coordinatively unsaturated iron atoms.[10,11] Synthetic three-coordinate iron compounds are expected to give insight into the reactivity of these special iron sites,[4] but only one synthetic three-coordinate iron complex actually reacts with N_2.[12]

A number of groups have reported that β-diketiminate ligands are adept at stabilizing three-coordination in main group and late transition metals.[13,14] However, the low-coordinate chemistry of iron, cobalt, and nickel with bulky β-diketiminates was unknown prior to our work.[15] The diketiminate ligand is ideal because it is difficult to displace (chelate effect; anionic), easily synthesized, and sterically enforces three-coordination *with only two donors*. For example, sufficiently large diketiminate ligands can stabilize a three-coordinate iron(II) complex with a synthetically versatile terminal chloride ligand.[16] We recently reported detailed electronic structure studies of this and other three-coordinate iron complexes using Mössbauer and EPR spectroscopy coupled with theoretical methods and mentioned the synthesis of the *first* three-coordinate methyl complex of the transition metals, $LFeCH_3$ [L = 2,2,6,6-tetramethyl-3,5-bis(2,6-diisopropylphenylimido)hept-4-yl, Figure 2].[17] The present contribution fully discloses the structure and properties of this 12-valence-electron iron(II) complex. More importantly, we show that the synthesis of stable trigonal-planar complexes can be extended to analogous three-coordinate cobalt(II) and nickel(II) chloride complexes and to a 13-electron cobalt(II) methyl complex. Interestingly, all five of the above chloride and methyl complexes have very similar solid-state structures, although the ability to create methyl complexes drastically changes through the series.

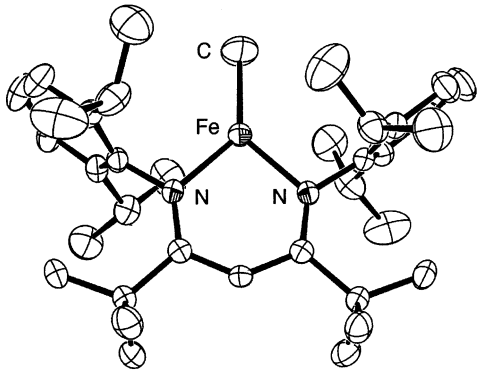

Figure 3. Plot of $LFeCH_3$ using 50% thermal ellipsoids. Hydrogen atoms are omitted for clarity.

Results

Synthesis, NMR Spectroscopy, and Stability of a 12-Electron Methyliron Complex. Treatment of ethereal solutions of LFeCl with methyl Grignard reagents yields pale orange crystalline $LFeCH_3$. This complex was briefly reported, but its solution behavior and solid-state structure have not been discussed.[17] Like its chloride precursor, $LFeCH_3$ is highly sensitive to air or moisture and was handled in a glovebox under purified nitrogen. This complex is thermally stable in solution, decomposing only after days in boiling C_6D_6. A representation of its X-ray crystal structure is shown in Figure 3; the two halves of the molecule are related by a crystallographic 2-fold axis that renders the FeN_2C unit rigorously planar. No agostic interactions of ligand C−H bonds are evident (Fe···H−C $\geq$ 2.78 Å), showing that it is a bona fide[4c] 12-electron organometallic complex. This trigonal planar metal geometry (approximately C_{2v}) is shared by all of the three-coordinate chloride and methyl complexes described below, because they all crystallize in the *same* space group ($C2/c$) with the same packing ($Z = 4$, rotation axis along b and through the M−Cl or M−C bond).

The proton NMR spectrum of $LFeCH_3$ shows resonances for all of the protons except the iron-bound methyl group.[18] The compound is paramagnetic (solution $\mu_{eff} = 5.5\ \mu_B$, $S = 2$), and the chemical shifts span a range of $\pm$150 ppm. The aryl groups are locked on the NMR time scale, as shown by the inequivalence of the two methyl groups of the isopropyl substituents.[19] The diketiminate proton resonances could be assigned using integration, leaving only two ambiguities: the inequivalent

(10) Selected recent biochemical work that supports binding of N_2 at Fe: (a) Lee, H.-I.; Sorlie, M.; Christiansen, J.; Song, R.; Dean, D. R.; Hales, B. J.; Hoffman, B. M. *J. Am. Chem. Soc.* **2000**, *122*, 5582−5587. (b) Christiansen, J.; Dean, D. R.; Seefeldt, L. C. *Annu. Rev. Plant Physiol. Plant Mol. Biol.* **2001**, *52*, 269−295. (c) Benton, P. M. C.; Mayer, S. M.; Shao, J.; Hoffman, B. M.; Dean, D. R.; Seefeldt, L. C. *Biochemistry* **2001**, *40*, 13816−13825. (d) Krahn, E.; Weiss, B. J. R.; Kröckel, M.; Groppe, J.; Henkel, G.; Cramer, S. P.; Trautwein, A. X.; Schneider, K.; Müller, A. *J. Biol. Inorg. Chem.* **2002**, *7*, 37−45.

(11) Examples of theoretical work on N_2 binding to the FeMoco: (a) Dance, I. *Chem. Commun.* **1998**, 523−530. (b) Siegbahn, P. E. M.; Westerberg, J.; Svensson, M.; Crabtree, R. H. *J. Phys. Chem. B* **1998**, *102*, 1615−1623. (c) Rod, T. H.; Nørskov, J. K. *J. Am. Chem. Soc.* **2000**, *122*, 12751−12763.

(12) Smith, J. M.; Lachicotte, R. J.; Pittard, K. A.; Cundari, T. R.; Lukat-Rodgers, G.; Rodgers, K. R.; Holland, P. L. *J. Am. Chem. Soc.* **2001**, *123*, 9222−9223.

(13) Bourget-Merle, L.; Lappert, M. F.; Severn, J. R. *Chem. Rev.* **2002**, *102*, in press.

(14) (a) Holland, P. L.; Tolman, W. B. *J. Am. Chem. Soc.* **1999**, *121*, 7270−7271. (b) Holland, P. L.; Tolman, W. B. *J. Am. Chem. Soc.* **2000**, *122*, 6331−6332. (c) Randall, D. W.; George, S. D.; Holland, P. L.; Hedman, B.; Hodgson, K. O.; Tolman, W. B.; Solomon, E. I. *J. Am. Chem. Soc.* **2000**, *122*, 11632−11648. (d) Jazdzewski, B. A.; Holland, P. L.; Pink, M.; Young, V. G., Jr.; Spencer, D. J. E.; Tolman, W. B. *Inorg. Chem.* **2001**, *40*, 6097−6107. (e) Spencer, D. J. E.; Aboelella, N. W.; Reynolds, A. M.; Holland, P. L.; Tolman, W. B. *J. Am. Chem. Soc.* **2002**, *124*, 2108−2109.

(15) (a) Four-coordinate nickel complexes of the protonated diketimine ligand: Feldman, J.; McLain, S. J.; Parthasarathy, A.; Marshall, W. J.; Calabrese, J. C.; Arthur, S. D. *Organometallics* **1997**, *16*, 1514−1516. (b) Power's group has recently created some three-coordinate cobalt and iron complexes using diketiminate ligands: Panda, A.; Stender, M.; Wright, R. J.; Olmstead, M. M.; Klavins, P.; Power, P. P. *Inorg. Chem.* **2002**, *41*, 3909−3916.

(16) Smith, J. M.; Lachicotte, R. J.; Holland, P. L. *Chem. Commun.* **2001**, 1542−1543.

(17) Andres, H.; Bominaar, E.; Smith, J. M.; Eckert, N. A.; Holland, P. L.; Münck, E. *J. Am. Chem. Soc.* **2002**, *124*, 3012−3025.

(18) Attempts to identify a resonance corresponding to the iron-bound methyl group included the synthesis of $LFeCD_3$, but no deuterium resonance could be located between $\pm$1500 ppm in ^2H NMR spectra. See: Reuben, J.; Fiat, D. *J. Am. Chem. Soc.* **1969**, *91*, 1242. It is likely that the methyl protons/deuterons are relaxed by the paramagnetic iron too quickly for observation.

(19) (a) Radzewich, C. E.; Guzei, I. A.; Jordan, R. F. *J. Am. Chem. Soc.* **1999**, *121*, 8673−8674. (b) Prust, J.; Stasch, A.; Zheng, W.; Roesky, H. W.; Alexopoulos, E.; Uson, I.; Boehler, D.; Schuchardt, T. *Organometallics* **2001**, *20*, 3825−3828.

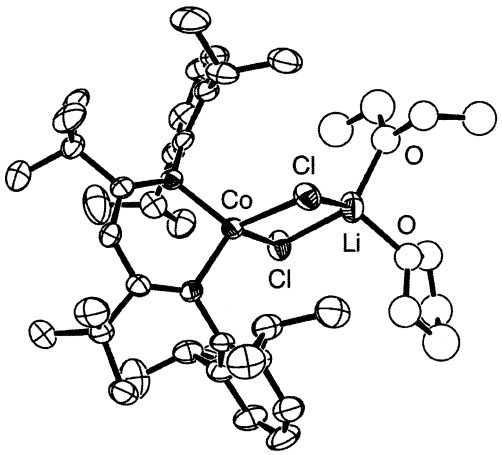

Figure 4. Plot of the major disorder component of $LCo(\mu\text{-}Cl)_2Li(ether)_2$ using 50% thermal ellipsoids. The minor component has two THF ligands coordinated to the lithium atom.

isopropyl methyl groups each integrate to 12, and the isopropyl methine and aryl protons meta to nitrogen each integrate to 4. Fortunately, the distances to the paramagnetic iron center (from the solid-state structure) differ greatly: the "front" (closer to X) isopropyl methyl protons are much closer (av 3.99 Å; closest 2.78 Å) than the "back" (closer to the backbone) methyl protons (av 5.53 Å; closest 5.14 Å), and the isopropyl methine protons are much closer (av 3.29 Å; closest 3.08 Å) than the aryl protons (av 5.18 Å; closest 5.14 Å). In each case, our assignments follow from correlating the distances to iron with (a) the shift of the peak and (b) the relaxation time. In general, the relaxation time was estimated from the peak broadness;[20] the accuracy of this method was confirmed by the measurement of similar (±1 ms) T_1 and T_2 values for each resonance of $LFeCH_3$.

Synthesis and Structure of Low-Coordinate Cobalt Chloride Complexes. Addition of a lithium β-diketiminate complex to a transition metal dihalide has been a general method for creation of three-coordinate iron(II) and copper(II) complexes.[14,16] We have shown that the additional bulkiness of the *tert*-butyl groups is necessary for restraining iron(II) to three-coordination.[16] However, addition of LLi(THF) to a slurry of $CoCl_2(THF)_{1.5}$ in THF yielded not LCoCl but dark brown $LCo(\mu\text{-}Cl)_2Li(ether)_2$, in 48% yield. This "ate" compound was characterized by X-ray crystallographic analysis (Figure 4). The best crystallographic model included two disorder components, one consisting of two THF ligands attached to lithium (minor) and the other containing THF and diethyl ether donors (major). The structure is well-ordered in the vicinity of the cobalt and diketiminate and, like other tetrahedral β-diketiminate complexes, has some folding of the MN_2C_3 ring into a "boat" conformation.[13,16,21]

Thallium(I) salts of ligands are often used in order to take advantage of the insolubility of TlCl as a driving force for formation of the desired complex (Scheme 1). Accordingly, treatment of $CoCl_2(THF)_{1.5}$ with LTl in THF gave the desired three-coordinate product LCoCl. Its X-ray crystal structure (Figure 5a) is virtually indistinguishable from that of LFeCl, and its metrical parameters will be discussed below. Crystals of LCoCl are strikingly dichroic, appearing purple or green depending on the direction of the transmitted light.

Scheme 1

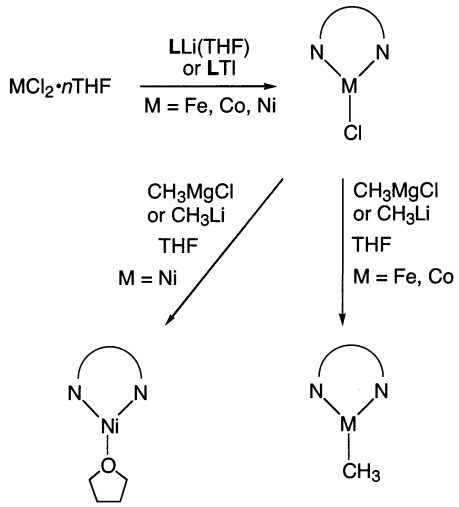

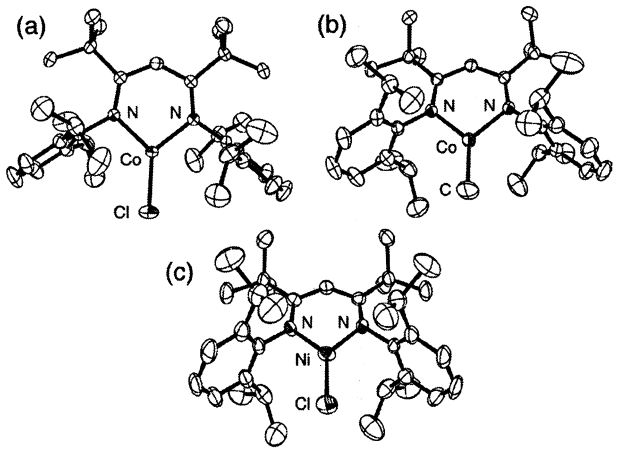

Figure 5. Plots of (a) LCoCl, (b) $LCoCH_3$, and (c) LNiCl using 50% thermal ellipsoids. Hydrogen atoms are omitted for clarity.

Both cobalt(II) complexes are high-spin, with solution magnetic moments of 4.7 μ_B that suggest an $S = 3/2$ ground state. The ^1H NMR spectra show paramagnetically shifted peaks that differ substantially by metal geometry. In tetrahedral $LCo(\mu\text{-}Cl)_2Li(ether)_2$, assignment of the broad, overlapping resonances was troublesome. On the other hand, resonances corresponding to all protons were reasonably sharp in the ^1H NMR spectrum of trigonal-planar LCoCl, and these could be assigned in the same way as in LFeCl and $LFeCH_3$ using integration, shift, and relaxation time. Most of the paramagnetic shifts are in the same direction as in the iron(II) analogues, with the most notable exception being the backbone vinyl resonance, which is at very high field in LCoCl and very low field in LFeCl.[16,36] The NMR analysis suggests that the solution structure of LCoCl is similar to that observed in the solid state.

A Three-Coordinate Methylcobalt Complex. The synthetic route to $LFeCH_3$ was also successful with Co(II): addition of methyl Grignard reagent to either $LCo(\mu\text{-}Cl)_2Li(ether)_2$ or

(20) Ming, L.-J. In *Physical Methods in Bioinorganic Chemistry*; Que, L., Ed.; University Science Books: Sausalito, CA, 2000. In rapidly tumbling small molecules, $T_2 \approx T_1$.

(21) Analysis of β-diketiminate distortion: (a) Stender, M.; Eichler, B. E.; Hardman, N. J.; Power, P. P.; Prust, J.; Noltemeyer, M.; Roesky, H. W. *Inorg. Chem.* **2001**, *40*, 2794−2799. (b) Hitchcock, P. B.; Lappert, M. F.; Layh, M. *J. Chem. Soc., Dalton Trans.* **2001**, 2409−2416. (c) MacAdams, L.; Kim, W.-K.; Liable-Sands, L. M.; Guzei, I. A.; Rheingold, A. L.; Theopold, K. H. *Organometallics* **2002**, *21*, 952−960. (d) Bailey, P. J.; Coxall, R. A.; Dick, C. M.; Fabre, S.; Parsons, S. *Organometallics* **2001**, *20*, 798−801. (e) Cheng, M.; Moore, D. R.; Reczek, J. J.; Chamberlain, B. M.; Lobkovsky, E. B.; Coates, G. W. *J. Am. Chem. Soc.* **2001**, *123*, 8738−8749.

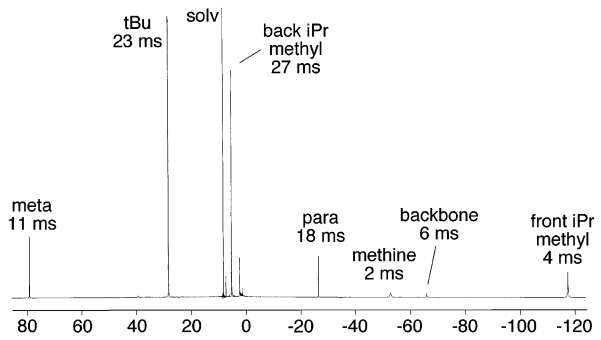

Figure 6. ^{1}H NMR spectrum (400 MHz) of a solution of $LCoCH_3$ in C_6D_6.

LCoCl gave good yields of the 13-electron organometallic complex $LCoCH_3$. Its solid-state structure is shown in Figure 5b, and metrical details are discussed below. The solution magnetic moment (4.9 μ_B) and proton NMR spectra were similar to those of LCoCl, strongly suggesting that it also has a high-spin d^7 configuration at cobalt. Again, all ligand hydrogen atoms are at least 2.8 Å from the cobalt atom, indicating that no direct electronic interaction between C−H bonds and the metal exists.

The stability of $LCoCH_3$ is greater than conventionally expected for an odd-electron organometallic complex,[22] especially one that is so electronically unsaturated. Heating solutions of $LCoCH_3$ in benzene at 80 °C gave slow decomposition over the course of a few days, but solutions were stable for long periods at room temperature (with rigorous exclusion of air and water).

It was possible to obtain well-resolved ^{1}H NMR spectra of $LCoCH_3$ that have paramagnetically shifted resonances (Figure 6). Integration and peak broadness (T_2) were again used to assign the resonances to specific sets of protons. Again the CH_3 resonance is not visible in $LCoCH_3$, nor is any ^{2}H resonance in $LCoCD_3$. As with LCoCl, the meta protons of the aryl substituents resonate further downfield, and the backbone proton of the diketiminate resonates much farther upfield, but the other resonances have paramagnetic shifts in the same direction as in $LFeCH_3$.

A Three-Coordinate Nickel(II) Chloride Complex. In analogy to the synthesis of LFeCl from $FeCl_2(THF)_{1.5}$ and $LLi(THF)$,[16] $NiCl_2(THF)_{0.7}$ was treated with the lithium diketiminate to give a deep green solution. While the three-coordinate iron(II) and cobalt(II) complexes were sensitive to oxidation by CH_2Cl_2, the nickel(II) complex could be crystallized from this solvent to give high yields of the three-coordinate complex LNiCl. The solution magnetic moment was 3.1 μ_B, consistent with an $S = 1$ ground state. Crystals were isomorphous with the three-coordinate iron and cobalt complexes, and a thermal-ellipsoid plot of the crystallographic model is shown in Figure 5c. The metrical parameters will be discussed below.

The proton NMR resonances were not as highly shifted as the above cobalt and iron compounds, with only the backbone resonance outside the range of +30 to −15 ppm. The relaxation times were 10−20 ms and did not constitute a good criterion for assigning peaks in the ^{1}H NMR spectrum. These relaxation times were too short to assign peaks using NOE spectroscopy, but DQF−COSY (see Supporting Information) showed correlations between the 4-proton peak at δ 29 and the other aryl resonance and between the 4-proton peak at δ 19 and the two isopropyl methyl resonances. These observations allow us to assign these two signals and confirm the assignments for the other signals (see Experimental Section).

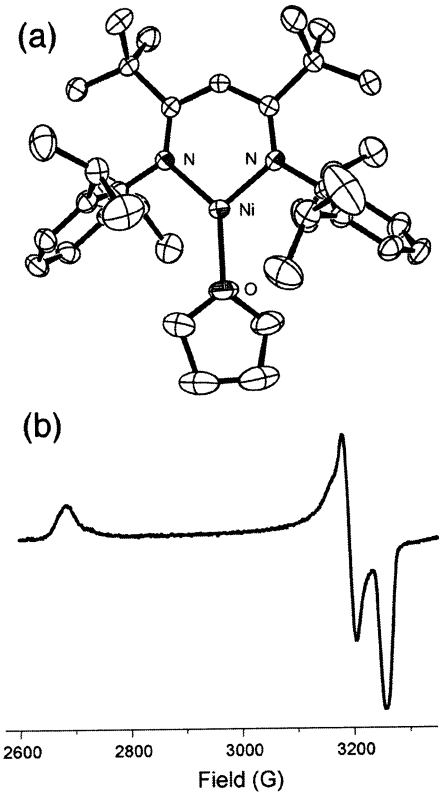

Figure 7. (a) Plot of LNi(THF) using 50% thermal ellipsoids. Hydrogen atoms are omitted for clarity. (b) X-band EPR spectrum of LNi(THF) in 2-methyltetrahydrofuran (77 K). Simulation yielded *g* values of 2.07, 2.11, and 2.51.

Attempted Alkylation of Nickel Gives Reduction to Nickel(I). Treatment of LNiCl with methyllithium or Grignard reagents did *not* give an alkylnickel(II) complex analogous to the iron(II) and cobalt(II) examples described above. Instead, a brown product was formed, the solid-state structure of which is shown in Figure 7a. The crystallographic analysis clearly shows that reduction occurred to give a nickel(I) diketiminate complex with solvent THF as the second ligand. The coordination of tetrahydrofuran is not irreversibly lost in pentane or diethyl ether solution, because crystals grown from these solvents retained THF. Support for the nickel(I) oxidation state comes from the solution magnetic moment (2.0 μ_B in THF-d_8) and a rhombic X-band EPR signal characteristic of an $S = 1/2$ system (Figure 7b).

$$LNiCl + CH_3Li + THF \rightarrow LNi(THF) + LiCl + CH_3\bullet \quad (1)$$

The reduction product LNi(THF) was observed even with bulky alkyllithium reagents such as neopentyllithium. To understand the mechanism of reduction, the reaction of LNiCl with methyllithium was studied in greater detail. The reaction is quite clean, with ^{1}H NMR spectra in THF-d_8 showing only the very broad resonances of LNi(THF) and sharp singlets at δ 0.86 and 0.18 corresponding to ethane and methane. Methyl radicals are expected as the product of methyl oxidation by nickel, and it is reasonable to propose that the ethane and

(22) Poli, R. *Chem. Rev.* **1996**, *96*, 2135−2204.

Table 1. Comparison of Calculated and Experimental Structures for Three-Coordinate Metal Chlorides[a]

		M–N (Å)	M–Cl (Å)	N–M–N (deg)
L′FeCl	($^5A_1$)	2.005	2.198	93.1
LFeCl		1.948(2)	2.172(1)	96.35(11)
L′CoCl	($^4A_2$)	1.952	2.178	94.0
LCoCl		1.902(2)	2.140(3)	99.49(13)
L′NiCl	($^3A_2$)	1.922	2.148	91.8
LNiCl		1.815(3)	2.137(2)	97.3(2)

[a] Calculated geometries (ground-state symmetry and multiplicity in parentheses) determined at the B3LYP/6-311+G(d) level of theory.

methane arise from coupling and hydrogen atom abstraction, respectively.

In an effort to trap a potential methylnickel complex through carbonyl insertion, the above reaction was repeated with an excess of CO or ^{13}CO gas. The reaction was cleanly diverted to a diamagnetic product. The ^{1}H and ^{13}C NMR spectra of an organic or organometallic $CH_3{}^{13}C(O)$-containing product from ^{13}CO insertion would show $^{13}C-{}^{13}C$ coupling in the ^{13}C spectrum and a doublet for the acyl group in the ^{1}H spectrum. Neither feature was observed, indicating that no irreversible CO insertion has taken place. The major product has two isopropyl resonances, characteristic of a diketiminate complex with C_{2v} symmetry (only one isopropyl environment; the two methyl groups are inequivalent, as discussed above). The high symmetry, diamagnetism, and the observation of a single isotopically sensitive carbonyl band (1938 cm^{-1}) in infrared spectra are most consistent with the nickel(0) complex $[LNi(CO)]^-$ as an assignment for the final product of the reaction of CH_3Li and LNiCl under CO, although conclusive characterization will require further study.

Comparative Computations on LMCl. Density functional B3LYP/6-311+G(d) calculations on L′MCl species (L′ = $C_3N_2H_5^-$) reveal a large manifold of states due to the small d-orbital splitting engendered by the low-coordination environment. Table 1 provides a comparison of the calculated L′MCl and experimental LMCl geometries. In general, the level of agreement between calculated and experimental structures is reasonable, apart from the discrepancy between the calculated (1.922 Å) and experimental (1.815(3) Å) Ni−N bond lengths. As discussed below, this difference is due to distortion of the ligand that was not possible in calculations constrained to the C_{2v} point group. The calculated N−M−N bite angles are systematically too small by approximately 5°. Test calculations on full models of L′FeCl ($^5A_1$) indicate that replacement of the appropriate H substituents in L′ with 2,6-diisopropylphenyl and *tert*-butyl increases the bite angle by 3°, and therefore, steric effects appear to be the main contributor to this systematic effect. This deviation should not detract from the trends that are analyzed below. The calculated differences in bite angles are small both in the computations as well as the experimental structures, but the trends are the same, i.e. the bite angle increases upon going from L′FeCl to L′CoCl and decreases from L′CoCl to L′NiCl.

Discussion

Three-Coordinate Complexes of Iron, Cobalt, and Nickel: Synthesis and Electronic Structures. Straightforward metathesis reactions with divalent metal halide salts appear to be a general route into three-coordinate complexes supported by β-diketiminate ligands. The complexes LMCl are distinctive among three-coordinate complexes because of the combination of the stable chelating diketiminate ligand and the easily substituted terminal halide ligand. Each of the LMCl complexes is the first characterized three-coordinate complex of its divalent metal with a terminal chloride ligand. As such, they offer a route into a systematic series of trigonal complexes with differing electronic properties and spectroscopic parameters.[17]

Solution susceptibility measurements suggest that all of the complexes have maximum spin multiplicity at room temperature. Comparative calculations on L′MCl (L′ = diketiminate with alkyl and aryl groups replaced with hydrogen) using restricted open-shell DFT under C_{2v} symmetry support the contention that high-spin configurations are lowest in energy. These electronic configurations are shown in Figure 9 below, with the *z* axis along the M−Cl bond. Interestingly, the two a_1-symmetry orbitals most closely approximate d_{x^2} and $d_{y^2-z^2}$ orbitals, in agreement with our description of three-coordinate iron(II) complexes derived from spectroscopic measurements.[17] The energy order of d orbitals is fairly consistent across the series of divalent metals from Mn (d^5) to Zn (d^{10}): d_{x^2}, $d_{xy} < d_{y^2-z^2}$, $d_{xz} < d_{yz}$. The d_{x^2} and d_{xy} orbitals are very close in energy, making two states ($^5A_1$ and $^5A_2$) energetically indistinguishable for L′FeCl; in the comparisons below, the spectroscopically determined $^5A_1$ state (d_{x^2} doubly occupied) is used.[17] In L′NiCl, the 4 kcal/mol energy difference favoring the $^3A_2$ state suggests double occupation of the $d_{y^2-z^2}$ rather than the d_{xz} orbital. Thus, the predicted ground-state terms for L′MCl are $^6A_1$ (Mn^{2+}), $^5A_1$ (Fe^{2+}), $^4A_2$ (Co^{2+}), $^3A_2$ (Ni^{2+}), $^2B_2$ (Cu^{2+}), and $^1A_1$ (Zn^{2+}). The calculated ground state for L′CuCl (a close relative of the recently synthesized LCuCl[14e]) agrees with that derived from theory and calculation for (diketiminate)Cu($SCPh_3$),[14c] using different axes.

Three-Coordinate Complexes of Iron, Cobalt, and Nickel: Geometric Structures. Detailed metrical comparisons are enabled by the fact that LFeCl, LCoCl, LNiCl, $LFeCH_3$, and $LCoCH_3$ all have the same crystal packing. Therefore, geometric differences between the complexes cannot come from the ubiquitous "crystal packing effects," and even small changes should be interpretable. Table 2 compares key bond distances and angles for the five LMX structures. Spencer et al. have isolated the copper(II) analogue LCuCl,[14e] but its crystal structure has not been reported.

The metal−ligand bond distances monotonically decrease from iron to cobalt to nickel, as expected from the atomic radii [$r_{ion}(Fe^{II}-T_d) = 0.77$ Å; $r_{ion}(Co^{II}-T_d) = 0.72$ Å; $r_{ion}(Ni^{II}-T_d) = 0.69$ Å]. The M−N distances are 0.025−0.028 Å longer in the methyl complexes, reflecting the greater polarizing ability of chloride that leads to a more electrophilic metal.

The monodentate chloride and methyl ligands are expected to accurately illustrate the effect of coordination number on the metal's covalent radius. Compared to literature complexes, the Co−Cl, Ni−Cl, Fe−C, and Co−C distances are amazingly short. Each M−Cl distance is about two standard deviations below the mean M−Cl distance in the Cambridge Structural Database.[23] The metal−carbon distances, at 2.01 Å or less, are

(23) Cambridge Structural Database and VISTA, October 2001 release. Allen, R. H.; Kennard, O. *Chem. Design Automation News* **1993**, *8*, 31−37. Histograms generated by VISTA are in the Supporting Information.

Table 2. Bond Length and Angle Comparison. X = Metal-bound C, Cl, or O

dist/angle	LFeCl	$LFeCH_3$	LCoCl	$LCoCH_3$	LNiCl	LNi(THF)	$LCo(\mu\text{-}Cl)_2Li(ether)_2$
M−N (Å)	1.948(2)	1.973(1)	1.902(2)	1.930(1)	1.815(3)	1.876(1) 1.882(1)	1.961(2) 1.968(2)
M−X (Å)	2.172(1)	2.009(3)	2.140(1)	1.963(3)	2.137(2)	2.000(1)	2.2942(9) 2.3023(9)
N−M−N (deg)	96.35(11)	94.85(8)	99.49(13)	98.24(7)	97.3(2)	100.46(6)	99.4(1)
N−M−X (deg)	131.83(5)	132.57(4)	130.25(6)	130.88(3)	131.4(1)	133.31(6) 126.21(6)	111.7−118.3
C−N−C (deg)	128.4(2)	128.56(1)	128.0(2)	128.6(1)	130.3(4)	126.4(1) 129.6(1)	124.8(3) 125.8(3)
fold/twist[a] (deg)	0.49(9)	0.49(6)	0.27(10)	0.38(6)	7.15(1)	1.16(9)	16.1(2)
N···N (Å)	2.90	2.91	2.90	2.92	2.72	2.89	3.00

[a] Angle between the least-squares N−C−C−C−N and N−M−N planes of the six-membered diketiminate−metal ring.

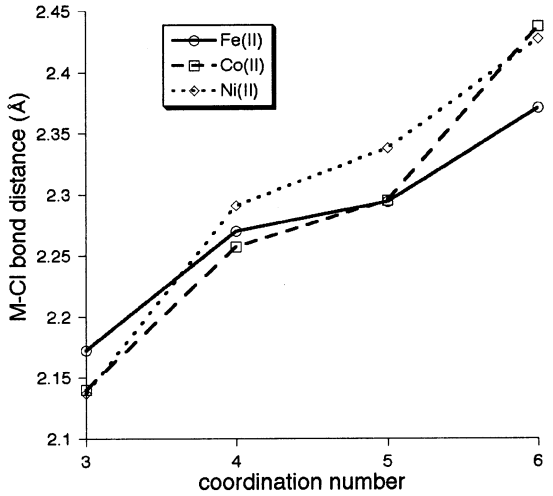

Figure 8. Mean metal−terminal chloride bond lengths for four- to six-coordinate complexes compared to the M−Cl bond lengths in three-coordinate LMCl. Mean bond lengths from VISTA analysis of the Cambridge Structural Database (Oct 2001).

especially notable: there is one shorter Fe−CH_3 bond,[24] and the only shorter Co−CH_3 bonds are in cobalt(III) complexes. The bond lengths to the small monodentate ligand can be used to illustrate the effect of coordination number on bond distances, unfettered by steric or chelate effects. For example, Figure 8 shows the trend in mean M^{II}−(terminal Cl) distances for iron, cobalt, and nickel in various coordination numbers, compared with our complexes, which are the first three-coordinate terminal chloride complexes of each metal in the +2 oxidation state.

Despite the extraordinarily low coordination number at the metal, the Fe−N and Co−N distances are only about one standard deviation shorter than the mean metal−N distance from the Cambridge Structural Database. However, the Ni−N distance is about *two* standard deviations shorter than the mean.[23] This suggests that the rigid diketiminate ligand is causing anomalous behavior in the iron and cobalt complexes; the reasons for this behavior will become clear below.

An interesting quantity is the "bite angle" of the ligand, defined as the N−M−N angle. There is no monotonic trend in this angle, which interestingly is maximum in the cobalt complex. The large N−Co−N angle implies that the diketiminate is more sterically congesting in LCoCl, which seems at odds with the greater tendency of LCoCl to attract lithium chloride in the synthesis of $LCo(\mu\text{-}Cl)_2Li(ether)_2$. The bite angle trend is also followed in the optimized theoretical models, suggesting that it is not a crystallographic artifact. There are two reasonable models through which one can explain the relative bite angles.

First, a close look at the crystal structures shows that, except for LNiCl, the distance between the two diketiminate nitrogen atoms (2.888−2.919 Å) is quite consistent in the LMX structures, despite the substantial changes in the bond distances. It is particularly notable that the N···N distance is 2.904 ± 0.001 Å in LFeCl and LCoCl, even though the Co−N bonds are shorter by 0.046 Å. Using a simple trigonometric model with a rigid diketiminate ligand, one can readily rationalize the change in bite angle because shorter bonds to a rigid chelating ligand must increase the angle (see Figure S-1). However, using a rigid diketiminate and the observed Ni−N distance of 1.815 Å, one predicts a N−Ni−N angle of about 106°. Presumably the complex avoids the poor metal−ligand orbital overlap in this planar geometry by distorting the diketiminate ring. The observed "twist" distortion maintains the crystallographically observed C_2 symmetry while bringing the nitrogen atoms about 0.018 Å closer together. In this model, the large N−Co−N angle represents maximum strain on the rigid planarity of the diketiminate backbone before it succumbs to distortion. This model also explains the exceptional ability of LCoCl to bind LiCl (see above): this strain is relieved by folding in the four-coordinate $LCo(\mu\text{-}Cl)_2Li(ether)_2$.

Reproduction of the bite angle trend in calculations in which C_{2v} symmetry is enforced (out-of-plane distortions are impossible) indicates that other factors may also affect the bite angle. In particular, an analysis of the frontier orbitals suggests that the metal d orbital configuration can play a role in determining the bite angle of β-diketiminate ligands. The d orbital manifold of L′MCl derived from the density functional calculations is depicted in Figure 9. From L′FeCl ($^5A_1$) to L′CoCl ($^4A_2$), an a_2 orbital that is primarily comprised of the metal d_{xy} is filled; from L′CoCl ($^4A_2$) to L′NiCl ($^3A_2$), an a_1 orbital ($\sim d_{y^2-z^2}$) is filled. Although these orbitals are primarily (~90%) metal in character, they do contain some ligand character, in particular that derived from the diketiminate nitrogen atoms. The ligand a_2 orbital is N···N antibonding, while the a_1 orbital is N···N bonding. Therefore, occupation of the a_2 and a_1 orbitals leads to an increase and decrease, respectively, in the bite angle.

Stability of High-Spin Methyl Complexes of the Late Metals. Low-coordinate alkyl complexes have been postulated as unobserved, reactive intermediates in C−H and C−C bond cleaving reactions.[25,26] Thus, it is surprising that the complexes $LMCH_3$ (Fe, 12-electron complex; Co, 13-electron complex)

(24) Balch, A. L.; Olmstead, M. M.; Safari, N.; St. Claire, T. N. *Inorg. Chem.* **1994**, *33*, 2815−2822.

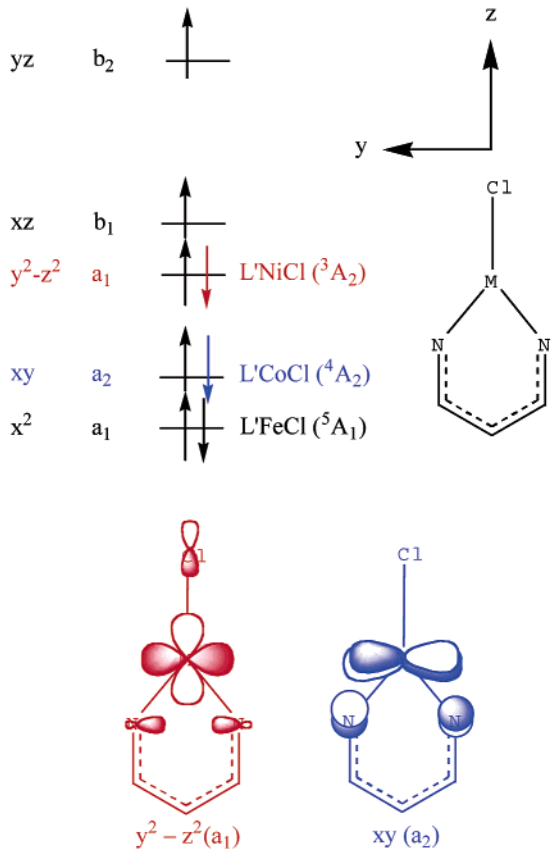

Figure 9. Frontier orbital diagram for L′MCl derived from density functional calculations. L′ = parent diketiminate ligand with no alkyl or aryl substituents.

are thermally stable in solution. In his review of open-shell organometallic complexes, Poli notes that many decomposition pathways are invalidated by the absence of *empty* d-orbitals in high-spin complexes,[22] a contention supported by the analogous stability of Parkin's 14-electron methyliron complex (PhTptBu)-$FeCH_3$.[27] Tris(pyrazolyl)borate and related ligands also lead to tetrahedral 15-electron cobalt(II)−methyl complexes.[28,29]

The reactivity of paramagnetic methylnickel complexes is also relevant to nickel-containing enzymes. Methylnickel intermediates have been postulated in the A cluster of acetyl-coenzyme A synthase.[30] Although a methylnickel intermediate is generally thought to be an intermediate in methanogenesis by methyl-coenzyme M reductase,[31] a very recent computational study suggests a mechanism with no methyl−nickel bond formation.[32] These considerations spurred us to attempt formation of $LNiCH_3$ by reactions analogous to those used to create $LFeCH_3$ and $LCoCH_3$, but ethane, methane, and a nickel(I) product were observed.

In one mechanistic possibility, $LNiCH_3$ is formed and then decomposes through homolysis to LNi and $CH_3^{\bullet}$. Observation of ethane as a byproduct strongly supports the formation of methyl radicals. Homolysis of $Ni^{II}-CH_3$ bonds is well-known,[33] and this facile decomposition pathway for high-spin organometallic complexes presumably is responsible for the absence of trigonal or tetrahedral nickel(II) methyl complexes in the literature.[28,33,34] Low-temperature ^1H NMR spectroscopy has been useful in observing nickel-containing intermediates,[35] but LNiCl is practically insoluble in THF at low temperatures. By briefly warming the solution and reintroducing it to the NMR probe at −80 °C, it was possible to observe an intermediate with resonances at δ 66 and −47 that builds up to very low concentration before converting to LNi(THF). Its peaks are relatively narrow but paramagnetically shifted, suggesting a high-spin Ni(II) formulation, but it could not be identified conclusively, and its concentration is low enough that other spectroscopic methods have not been pursued.

In the absence of direct spectroscopic evidence, we sought to trap $LNiCH_3$ by thawing the THF solution under an atmosphere of carbon monoxide. Insertion of CO into the Fe−C bond of the analogue $LFeCH_3$ is rapid.[36] However, attempted alkylation of LNiCl under carbon monoxide yielded a product tentatively assigned as $[LNi(CO)]^-$. With no evidence to support transient formation of $LNiCH_3$, we must conclude that the simplest reasonable mechanism, electron transfer from CH_3Li to LNiCl followed by LiCl formation and THF coordination to nickel, is operative.

Conclusions

This report shows that β-diketiminate ligands offer a general route to robust three-coordinate complexes of group 8, 9, and 10 metals. The three-coordinate complexes are unusual in that one of the ligands can be small, and this ligand may be substituted easily. The steric protection even stabilizes highly electronically unsaturated organometallic complexes, and thus it has been possible to synthesize the first two three-coordinate methyl complexes of the transition metals. Detailed structural comparison of five isomorphous three-coordinate complexes, in combination with theory, has given us preliminary insights into their electronic structure, a subject of future detailed spectroscopic studies. Finally, systematic comparison has shown that paramagnetic nickel(II)−alkyl complexes are not formed with the method that generates stable iron(II) and cobalt(II)

(25) Recent examples: (a) Plutino, M. R.; Scolaro, L. M.; Romeo, R.; Grassi, A. *Inorg. Chem.* **2000**, *39*, 2712−2720. (b) Gandelman, M.; Vigalok, A.; Konstantinovski, L.; Milstein, D. *J. Am. Chem. Soc.* **2000**, *122*, 9848−9849. (c) Kanzelberger, M.; Singh, B.; Czerw, M.; Krogh-Jespersen, K.; Goldman, A. S. *J. Am. Chem. Soc.* **2000**, *122*, 11017−11018. (d) Crumpton, D. M.; Goldberg, K. I. *J. Am. Chem. Soc.* **2000**, *122*, 962−963. (e) Fekl, U.; Goldberg, K. I. *J. Am. Chem. Soc.* **2002**, *124*, 6804−6805. (f) Review: Stahl, S. S.; Labinger, J. A.; Bercaw, J. E. *Angew. Chem., Int. Ed. Engl.* **1998**, *37*, 2180−2192.
(26) Recent evidence suggests that associative mechanisms without three-coordinate intermediates may be more reasonable in some cases: (a) Cao, Z.; Hall, M. B. *Organometallics* **2000**, *19*, 3338−3346. (b) Johansson, L.; Tilset, M. *J. Am. Chem. Soc.* **2001**, *123*, 739−740. (c) Zhong, H. A.; Labinger, J. A.; Bercaw, J. E. *J. Am. Chem. Soc.* **2002**, *124*, 1378−1399. (d) Procelewska, J.; Zahl, A.; van Eldik, R.; Zhong, H. A.; Labinger, J. A.; Bercaw, J. E. *Inorg. Chem.* **2002**, *41*, 2808−2810.
(27) Kisko, J. L.; Hascall, T.; Parkin, G. *J. Am. Chem. Soc.* **1998**, *120*, 10561−10562.
(28) Schebler, P. J.; Mandimutsira, B. S.; Riordan, C. G.; Liable-Sands, L. M.; Incarvito, C. D.; Rheingold, A. L. *J. Am. Chem. Soc.* **2001**, *123*, 331−332.
(29) Jewson, J. D.; Liable-Sands, L. M.; Yap, G. P. A.; Rheingold, A. L.; Theopold, K. H. *Organometallics* **1999**, *18*, 300−305.
(30) Recent discussions: Lindahl, P. A. *Biochemistry* **2002**, *41*, 2097−2105. (b) Seravalli, J.; Kumar, M.; Ragsdale, S. W. *Biochemistry* **2002**, *41*, 1807−1819.
(31) (a) Ermler, U.; Grabarse, W.; Shima, S.; Goubeaud, M.; Thauer, R. K. *Science* **1997**, *278*, 1457−1462. (b) Horng, Y.-C.; Becker, D. F.; Ragsdale, S. W. *Biochemistry* **2001**, *40*, 12875−12885.
(32) Pelmenschikov, V.; Blomberg, M. R. A.; Siegbahn, P. E. M.; Crabtree, R. H. *J. Am. Chem. Soc.* **2002**, *124*, 4039−4049.
(33) (a) Jolly, P. W.; Jonas, K.; Krueger, C.; Tsay, Y. H. *J. Organomet. Chem.* **1971**, *33*, 109−122. (b) D'Aniello, M. J.; Barefield, E. K. *J. Am. Chem. Soc.* **1976**, *98*, 1610−1611.
(34) Diamagnetic square-planar complexes of nickel(II) are common.
(35) A recent example: Shultz, C. S.; DeSimone, J. M.; Brookhart, M. *J. Am. Chem. Soc.* **2001**, *123*, 9172−9173.
(36) Smith, J. M.; Lachicotte, R. L.; Holland, P. L. *Organometallics* **2002**, *21*, 4808−4814.

analogues, an observation that may be relevant to the mechanism of enzymatic methanogenesis.

Experimental Section

General Considerations. All manipulations were performed under a nitrogen atmosphere by standard Schlenk techniques or in an M. Braun Unilab N_2-filled glovebox maintained at or below 1 ppm of O_2 and H_2O. Glassware was dried at 150 °C overnight. Proton NMR data were recorded on Bruker Avance 400 or Bruker AMX-400 spectrometers (400 MHz) at 22 °C. Shifts are reported in ppm, relative to residual protiated solvent in C_6D_6 (δ 7.15), CH_2Cl_2 (δ 5.31), or THF-d_8 (δ 1.73, 3.58). In parentheses are listed: integrations, T_2 values in ms calculated as $(\pi\Delta\nu_{1/2})^{-1}$,[20] and assignments. Carbon-13 NMR spectra of the paramagnetic compounds showed substantially fewer peaks than expected and were not pursued. T_1 measurements and DQF−COSY were recorded on a Varian INOVA-500 spectrometer (500 MHz) at 30.0 °C; T_1 values were calculated using a curve-fitting procedure.[37] IR spectra were recorded on a Mattson Instruments 6020 Galaxy Series FTIR; solution spectra used a cell with CsF windows. EPR spectroscopy at 77 K used a quartz Dewar suspended in the cavity of a Bruker ESP-300 spectrometer; parameters are given in the Supporting Information. UV−vis spectra were measured on a Cary 50 spectrophotometer, using cuvettes sealed to a Schlenk-type stopcock. Solution magnetic susceptibilities were determined by Evans' method,[38] and are considered accurate to $\pm 0.3\ \mu_B$. Microanalysis was performed by Desert Analytics (Tucson, AZ).

Pentane, diethyl ether, methylene chloride, tetrahydrofuran (THF), and toluene were purified by passage through activated alumina and "deoxygenizer" columns from Glass Contour Co. (Laguna Beach, CA). Deuterated benzene, THF-d_8, and 2-methyltetrahydrofuran were dried over CaH_2 and then over Na and then vacuum distilled into a storage container or directly into the NMR tube. Carbon monoxide (CP grade) was obtained from Air Products, and ^{13}CO (99 atom %) was from Aldrich Chemical Co. Anhydrous metal salts were prepared by treatment of the hydrates with thionyl chloride.[39] The $MCl_2(THF)_n$ complexes were prepared using the method of Kern,[40] and $NiCl_2$ was converted to a THF adduct using an analogous method.[41] Celite was dried at 200 °C under vacuum. The lithium salt LLi(THF) was prepared by treating a solution of LH[42] in THF with 1.0 equiv of butyllithium, removing solvent, and crystallizing from pentane. Methyllithium (Aldrich, 1.4 M in diethyl ether) was transferred in a 8−10 mL portion to a 20-mL scintillation vial, treated with several drops of dioxane to precipitate halide impurities,[43] filtered through Celite, and pumped down to a white solid for use. Methylmagnesium chloride (Aldrich, 3 M in THF) was used as received. The preparation of LFeCl and $LFeCH_3$ has been described previously.[16,17] A solution of CD_3MgI for the preparation of $LFeCD_3$ and $LCoCD_3$ was generated by stirring a solution of CD_3I (Aldrich) in diethyl ether with Mg metal. Methyl-d_3 compounds synthesized from this Grignard reagent solution were spectroscopically identical to their protiated analogues.

Assignment of ^{1}H NMR Signals in $LFeCH_3$.[17] [shift in ppm (integration, T_1 in ms, T_2 in ms, assignment)] δ 133.2 (1, <1, 0.4, backbone), 42.8 (18, 2, 2, tBu), −3.1 (4, 6, 5, *m*-aryl), −28.3 (12, 6, 5, "back" ^{i}Pr methyl), −108.1 (2, 4, 3, *p*-aryl), −118.2 (4, <1, 0.2, ^{i}Pr methine), −129.5 (12, <1, 0.4, "front" ^{i}Pr methyl).

LCo(μ-Cl)$_2$Li(ether)$_2$. A solution of LLi(THF) (722 mg, 1.24 mmol) in THF (5 mL) was added to a slurry of $CoCl_2(THF)_{1.5}$ (291 mg, 1.22 mmol) in THF (5 mL) and stirred for 4 h. Volatile materials were removed from the dark green mixture under vacuum, and the residue was extracted with 2:1 diethyl ether/pentane (17 mL), filtered, and concentrated to 8 mL. Cooling to −35 °C gave brown crystals of $LCo(\mu\text{-}Cl)_2Li(ether)_2$ (458 mg, 48% yield). ^{1}H NMR (400 MHz, C_6D_6): δ 50 (br), 22.2, 20 (br), 12.0, 8.8, 3.8, 2.1, 1.5, 0.4, −7, −40, −43. μ_{eff} (C_6D_6, 295 K)= 4.7 μ_B. IR (toluene): 1619 (w), 1535 (m), 1492 (s), 1432 (m), 1384 (vs), 1362 (vs), 1317 (vs), 1217 (m), 1102 (w), 1049 (m) cm^{-1}. UV−vis (toluene, ϵ in mM^{-1} cm^{-1}): 338 (12), 512 (0.50), 538 (0.47), 689 (0.40) nm. Anal. Calcd for $C_{43}H_{71}N_2O_2CoLiCl_2$: C, 65.81, H, 9.12, N, 3.57. Found: C, 65.86, H, 9.02, N, 3.35.

LTl. LLi(THF) (742 mg, 1.28 mmol) was added to a stirred solution of thallium ethoxide (Aldrich, 319 mg, 1.28 mmol) in pentane (13 mL). After several hours, the yellow mixture was pumped down, extracted with toluene (60 mL), and filtered. Volatile materials were removed from the filtrate, and the residue was washed with cold pentane to give 550 mg (61% yield) of yellow powder. This powder appeared pure by NMR spectroscopy, but sensitivity to trace air or to light prevented trustworthy elemental analysis (the material turned black in transit). ^{1}H NMR (400 MHz, C_6D_6): δ 7.03(m, 6, aryl), 5.31(s, 1, backbone), 3.34 (septet, 4, ^{i}Pr), 1.29(d, 12, ^{i}Pr), 1.27(s, 18, tBu), 1.2(br s, 12, ^{i}Pr). ^{13}C NMR (400 MHz, C_6D_6): δ 169.7, 140.3, 123.6, 33.2, 27.7, 23.2. IR (toluene): 1533 (m), 1390 (s), 1366 (m), 1327 (w), 1218 (w), 1146 (w), 1096 (w) cm^{-1}. UV−vis (toluene, ϵ in mM^{-1} cm^{-1}): 376(18) nm. A preliminary X-ray crystal structure showed monomeric LTl but had apparent twinning problems that prevented accurate solution of the structure.

LCoCl. A solution of LTl (126 mg, 0.178 mmol) in THF (5 mL) was added to a slurry of $CoCl_2(THF)_{1.5}$ (42 mg, 0.176 mmol) in THF (5 mL), stirred for 2.5 h, and then filtered. Volatile materials were removed to leave a brown residue that was dissolved in diethyl ether (2 mL). Crystals formed upon standing at room temperature for several hours. Total yield: 42 mg (40%). ^{1}H NMR (400 MHz, C_6D_6): δ 60.8 (4, 4, *m*-aryl), 27.6 (18, 5, tBu), −2.8 (12, 6, ^{i}Pr "back" methyl), −46.0 (2, 6, *p*-aryl), −57.4 (4, 1, ^{i}Pr methine), −84.4 (12, 2, ^{i}Pr "front" methyl), −90.7 (1, 3, backbone). μ_{eff} (C_6D_6, 295 K) = 4.7 μ_B. UV−vis (toluene, ϵ in mM^{-1} cm^{-1}): 358(6.8), 510 (sh, ∼0.2), 652 (0.10) nm. Mp: 240 °C (dec). Anal. Calcd for $C_{35}H_{53}N_2CoCl$: C, 70.51, H, 8.96, N, 4.70. Found: C, 69.30, H, 9.12, N, 4.81.

$LCoCH_3$. Methylmagnesium chloride (0.12 mL, 0.36 mmol) was added to a solution of $LCo(\mu\text{-}Cl)_2Li(ether)_2$ (216 mg, 0.276 mmol) in diethyl ether (7 mL), leading to immediate formation of a white precipitate. After 0.5 h, the mixture was filtered, volatile materials were removed from the filtrate under vacuum, and the residue was extracted with 1:1 diethyl ether/pentane (20 mL). The solution was concentrated to 8 mL, filtered, and cooled to −35 °C to give brown crystals of $LCoCH_3$. ^{1}H NMR (400 MHz, C_6D_6): δ 78.1 (4, 11, *m*-aryl), 27.2 (18, 23, tBu), 4.1 (12, 27, ^{i}Pr "back" methyl), −27.6 (2, 18, *p*-aryl), −53.8 (4, 2, ^{i}Pr methine), −67.1 (1, 6, backbone), −118 (12, 4, ^{i}Pr "front" methyl). μ_{eff} (C_6D_6, 295 K) = 4.9 μ_B. IR (toluene): 1511 (m), 1433 (m), 1383 (vs), 1363 (vs), 1319 (s), 1220 (m), 1198 (w), 1098 (w) cm^{-1}. UV−vis (toluene, ϵ in mM^{-1} cm^{-1}): 335(15), 565(0.13), 725(0.16) nm. Anal. Calcd for $C_{36}H_{56}CoN_2$: C, 75.10, H, 9.80, N, 4.87. Found: C, 74.78, H, 9.68, N, 4.80.

LNiCl. A Schlenk flask was loaded with $NiCl_2(THF)_{0.7}$ (1.75 g, 10.2 mmol), LLi(THF) (3.72 g, 6.41 mmol), and THF (30 mL) and heated to 70 °C overnight. Volatile materials were removed from the dark green mixture under vacuum, and the residue was extracted with CH_2Cl_2 (70 mL), filtered, and concentrated to 15 mL. Addition of diethyl ether (10 mL) and cooling to −35 °C gave green crystals of LNiCl. A second crop of crystals was collected to give a total yield of 2.5 g (66%).^{1}H NMR (400 MHz, CD_2Cl_2): δ 29.3 (4, 14, *m*-aryl), 18.5 (4, 11, ^{i}Pr methine), 5.6 (12, 19, ^{i}Pr methyl), 4.1 (12, 18, ^{i}Pr methyl), 2.5 (18, 21, tBu), −14.7 (2, 14, *p*-aryl), −123.5 (1, 11, backbone). μ_{eff} (CD_2Cl_2, 295 K) = 3.1 μ_B. IR (CH_2Cl_2): 2967 (vs), 2869 (m), 1587 (w), 1521

(37) Evaluation of T_1 from an inversion−recovery experiment is described: Levy, G. C.; Peat, I. R. *J. Magn. Reson.* **1975**, *18*, 500−521.
(38) Schubert, E. M. *J. Chem. Educ.* **1992**, *69*, 62.
(39) Pray, A. R. *Inorg. Synth.* **1990**, *28*, 321−323.
(40) Kern, R. J. *J. Inorg. Nucl. Chem.* **1962**, *24*, 1105−1109.
(41) Eckert, N. A.; Bones, E. M.; Lachicotte, R. L.; Holland, P. L., submitted.
(42) Budzelaar, P. H. M.; van Oort, A. B.; Orpen, A. G. *Eur. J. Inorg. Chem.* **1998**, 1485−1494.
(43) Holland, P. L.; Smith, M. E.; Andersen, R. A.; Bergman, R. G. *J. Am. Chem. Soc.* **1997**, *119*, 12815−12823.

(m), 1464 (m), 1385 (m), 1366 (s), 1315 (s), 1268 (vs), 1221 (w), 1099 (w), 1057 (w) cm^{-1}. UV−vis (CH_2Cl_2, ϵ in mM^{-1} cm^{-1}): 372 (8.4), 467 (sh, 1.7), 838 (1.4) nm. Anal. Calcd for $C_{35}H_{53}N_2NiCl$: C, 70.54, H, 8.96, N, 4.70. Found: C, 69.25, H, 9.02, N, 4.63.

LNi(THF). A mixture of LNiCl (295 mg, 0.495 mmol) and CH_3Li (14 mg, 0.64 mmol) was dissolved in THF (10 mL). After stirring the orange solution for 2 h, volatile materials were removed. The residue was extracted with pentane (10 mL), filtered, and reduced to 6 mL under vacuum. Cooling to −35 °C gave brown crystals of LNi(THF). A second crop was also collected, for a total yield of 0.18 g (58%). ^{1}H NMR (400 MHz, THF-d_8): δ 24 (sh), 21.5, 20 (sh), 12.5, 3.9, −1.8, −11.5, −50 (sh); there was also a noticeable lump in the baseline from about +60 to −60 ppm, suggesting that other resonances are too broad to be observed as peaks. μ_{eff} (THF-d_8, 295 K) = 2.0 μ_B. EPR (9.425 GHz, 77K, MeTHF): g = 2.068, 2.11, 2.51. IR (Nujol): 1504 (s), 1427 (s), 1402 (vs), 1366 (s), 1322 (s), 1220 (m), 1152 (m), 1097 (m) cm^{-1}. UV−vis (THF, ϵ in mM^{-1} cm^{-1}): 310 (25), 412 (5.8), 428 (5.5), 485 (1.8), 520 (sh, 1.5) nm. Anal. Calcd for $C_{39}H_{61}N_2NiO$: C, 74.05, H, 9.72, N, 4.43. Found: C, 73.66, H, 9.53, N, 4.76.

Reaction of LNiCl with CH_3Li. Roughly 15 mg of LNiCl and 2 mg of CH_3Li were placed in a J. Young NMR tube, and THF-d_8 (0.8 mL) was condensed into the tube at 77 K. At −80 °C, the chloride complex does not dissolve in THF, but brief warming caused the liquid phase to change to a light orange color. The tube was immediately cooled to −80 °C for several minutes. ^{1}H NMR spectroscopy at −80 °C showed the presence of starting materials, products, and additional peaks at δ 66 and −47 ppm. Warming the solution to room temperature for several minutes caused these two peaks to disappear, and in the final mixture only LNi(THF), excess CH_3Li, ethane, and methane (see below) were detectable by ^{1}H NMR.

Spectroscopic Yield and Detection of Byproducts. A mixture of solid LNiCl (22 mg, 0.037 mmol) and solid CH_3Li (0.8 mg, 0.04 mmol) was placed in a J. Young NMR tube, and THF-d_8 (0.6 mL) was condensed into the tube at 77 K. Warming gave a deep orange solution. The ^{1}H NMR spectrum of this solution was indistinguishable from that of LNi(THF), except for singlets at δ 0.86 and 0.18 ppm. The volatile materials were vacuum-distilled into another NMR tube. The ^{1}H NMR spectrum of the colorless distillate consisted of solvent peaks, trace water, and singlets at δ 0.86 and 0.18 ppm.

Trapping with CO. The reaction of LNiCl and CH_3Li was performed as above, but 1 atm of carbon monoxide was admitted into the tube before thawing the mixture. Warming gave an orange-yellow solution that was analyzed spectroscopically. **DANGER**: A small amount of $Ni(CO)_4$ may be produced in this reaction, and the reaction mixture should be handled with care in a fume hood. IR (THF solution): 1968, 1938 cm^{-1} (with ^{13}CO: 1966, 1893 cm^{-1}). ^{1}H NMR (400 MHz, THF-d_8): δ 6.91 (d, 4, *m*-aryl), 6.80 (t, 2, *p*-aryl), 4.94 (s, backbone), 3.24 (septet, 4, ^{i}Pr methine), 2.27 (s, 2−3, unassigned), 1.26 (d, 12, ^{i}Pr methyl), 1.14 (s, 18, tBu), 1.01 (d, 12, ^{i}Pr methyl).

X-ray Crystallography. Crystals or shards of crystals were mounted under Paratone-8277 on a glass fiber and placed in a cold nitrogen stream at −80 °C on the X-ray diffractometer. The X-ray intensity data were collected on a standard Siemens SMART CCD Area Detector System equipped with a normal focus molybdenum-target X-ray tube operated at 2.0 kW (50 kV, 40 mA). A total of 1321 frames of data (1.3 hemispheres) were collected using a narrow frame method with scan widths of 0.3° in ω and exposure times of 30−60 s/frame using a detector-to-crystal distance of 5.09 cm (maximum 2θ angle of 56.6°). Peaks were integrated to a maximum 2θ angle of 56.5° with the Siemens SAINT program. The final unit cell parameters (at −80 °C) were determined from the least-squares refinement of three-dimensional centroids of up to 8192 intense reflections. The data were corrected for absorption with the SADABS program.

Space groups were assigned using the XPREP program. The structures were solved using direct methods and refined employing full-matrix least-squares on F^2. All nonhydrogen atoms were refined with anisotropic thermal parameters. Hydrogen atoms were included in idealized positions with riding thermal parameters. Details on each structure may be found in the Supporting Information.

Computational Methods. Calculations were carried out using the Gaussian program.[44] The all-electron 6-311+G(d) basis set was used in conjunction with the B3LYP hybrid functional for all calculations described herein. The restricted Kohn−Sham formalism was used. Geometry optimizations were carried out within C_{2v} symmetry.

Acknowledgment. P.L.H. thanks the University of Rochester and the National Science Foundation (CHE-0134658) for funding. L.L.P. thanks REACH and NSF-REU (CHE-9987991) for summer support. T.R.C. acknowledges the National Science Foundation (CHE-9983665) for partial support of this research. We thank Phil Power for sharing ref 15b prior to publication, Emile Bominaar for insightful discussions, and Jeremy Smith for synthesizing $NiCl_2(THF)_{0.7}$ as well as helpful criticism. We are indebted to Brandy Russell and Kara Bren for help with T_1 measurements, to Sandip Sur for assistance with NMR spectroscopy, and to an anonymous reviewer for suggesting methyltetrahydrofuran as a solvent for EPR spectroscopy.

Supporting Information Available: Bond length comparisons from the Cambridge Structural Database, EPR spectrum of LNi(THF), DQF−COSY spectra of LNiCl, DFT optimized geometries for L′MCl, and crystallographic information files. This material is available free of charge via the Internet at http://pubs.acs.org.

JA025583M

(44) Frisch, M. J.; Trucks, G. W.; Schlegel, H. B.; Scuseria, G. E.; Robb, M. A. Cheeseman, J. R.; Zakrzewski, V. G.; Montgomery, J. A., Jr.; Stratmann, R. E.; Burant, J. C.; Dapprich, S.; Millam, J. M.; Daniels, A. D.; Kudin, K. N.; Strain, M. C.; Farkas, O.; Tomasi, J.; Barone, V.; Cossi, M.; Cammi, R.; Mennucci, B.; Pomelli, C.; Adamo, C.; Clifford, S.; Ochterski, J.; Petersson, G. A.; Ayala, P. Y.; Cui, Q., Morokuma, K.; Malick, D. K.; Rabuck, A. D.; Raghavachari, K.; Foresman, J. B.; Cioslowski, J.; Ortiz, J. V.; Stefanov, B. B.; Liu, G.; Liashenko, A.; Piskorz, P.; Komaromi, I.; Gomperts, R.; Martin, R. L.; Fox, D. J.; Keith, T.; Al-Laham, M. A.; Peng, C. Y.; Nanayakkara, A.; Gonzalez, C.; Challacombe, M.; Gill, P. M. W.; Johnson, B.; Chen, W.; Wong, M. W.; Andres, J. L.; Gonzalez, C.; Head-Gordon, M.; Replogle, E. S.; Pople, J. A. *GAUSSIAN*; Gaussian, Inc.: Pittsburgh, PA, 1998.